Voltammetric Study on the Transport of Ions of Various Hydrophobicity Types through Bilayer Lipid Membranes Composed of Various Lipids

Osamu Shirai,[#] Yumi Yoshida, Masakazu Matsui, Kohji Maeda,[†] and Sorin Kihara[*,†]

Institute for Chemical Research, Kyoto University, Uji, Kyoto 611

†Department of Chemistry, Kyoto Institute of Technology, Matsugasaki, Sakyo-ku, Kyoto 606

(Received April 24, 1996)

The ion transport from one aqueous medium, W1, to another, W2, through a bilayer lipid membrane, BLM, was investigated voltammetrically by scanning the applied membrane potential, ΔV_{W1-W2}, and monitoring the membrane current, I_{W1-W2}. The shapes of voltammograms observed with a definite BLM depended on the hydrophobicity and the concentration of the ion added into W1 and/or W2, and can be classified into four types. The transport processes involved in each type of voltammogram were elucidated in the light of knowledge about ion transport processes through liquid membranes and by taking into account the conjugated ion transfers at interfaces of W1/BLM and BLM/W2. The shapes of voltammograms were also transformed when BLMs made of different lipids were employed. The spontaneous condensation of objective ions from W1 and/or W2 to the BLM by the partition with counter ions, which depends on the properties of objective ions, counter ions and lipids composing BLMs, is essential for the ion transport through BLMs.

The ion transport from one aqueous medium, W1, to another, W2, through a bilayer lipid membrane, BLM, has been investigated extensively for the fundamental understanding of ion transfers through biomembranes.[1,2]

Though a BLM represents a high energy barrier for hydrophilic ions such as K^+, Na^+, or Cl^-,[3,4] the ion transport occurs easily when a hydrophobic ion is added into W1 and/or W2 in the presence of hydrophilic salts, even if the additive is fairly dilute (e.g., 10^{-6} M, 1 M= 1 mol dm^{-3}).[5—7] The mechanism and energetics of the ion transport in the presence of the hydrophobic ion have been discussed frequently.[8—11] Most authors[5,6,8] assumed the condensation of the hydrophobic ion into the BLM, and attributed the rate-determining process to the diffusion-controlled mass transfer of the hydrophobic ion from the bulk of the aqueous medium, W, to the W/BLM interface when the hydrophobic ion was dilute. When the concentration of the hydrophobic ion was high, Le Blanc[8] considered the saturation of the space charge in the BLM with the ion, Bruner[9] and Ketterer et al.[10] the saturation of the interface by the adsorption of the ion, and De Levie and Seidah[11] the variation of concentration of the ion in the stagnant (Nernst) and space charge (Gouy–Chapman) layers in W due to the partition equilibrium or the first-order phase transfer kinetics at the W/BLM interface.

If we adopt the diffusion-controlled process in case of the dilute hydrophobic ion, however, it is difficult to explain not only the extraordinarily large current caused by the ion transport (10 to 100 times larger than the ordinary diffusion-controlled current) but also the cyclic voltammogram symmetrical about the origin (point of 0 V and 0 A) which is observed by scanning the membrane potential (potential difference between W1 and W2) and measuring the membrane current (current between W1 and W2) with the BLM system in the presence of hydrophobic ion in one of two aqueous phases. In order to overcome these difficulties, Kutnik and Tien[12] considered the transfer of hydrophobic ion, which had been concentrated in the BLM, from the BLM to both W1 and W2, and applied the thin layer electrode theory to the analysis of the voltammogram.

Reviewing previous works on the transport process, we find that the role of the hydrophilic ions in aqueous phases which must be distributed into the BLM together with the hydrophobic ion as the counter ion in order to hold the electroneutrality in the membrane and aqueous phases has not been taken into account. Hence it seems difficult to understand the different feature of the ion transport observed by varying the kind or concentration of hydrophilic salts based on the concepts so far proposed.

The present authors compared the voltammogram for ion transport through a BLM with that through a liquid membrane in a previous paper,[13] and pointed out briefly that the hydrophilic ion moves into the BLM spontaneously as the counter ion of the hydrophobic ion; not the hydrophobic ion but the hydrophilic ion transfers between W1 and W2.

In the present work, voltammograms for transports of various ions through BLMs of various compositions are investigated. Then, processes involved in the transports are elucidated on the basis of the results of the previous work, taking into account solution chemical properties of the transferring

Present address: Japan Atomic Energy Research Institute, Oarai, Ibaraki 311-13.

ion, the coexisting ion, and the constituents of the BLM.

Experimental

Chemicals. Lipids used to form BLM are lecithin (Merck, No. 544274), (PC), which is a mixture of phosphatidylcholines with different aliphatic groups, dioleoylphosphatidylcholine (Wako Pure Chemical Ind., Ltd., No. 166-12803), (DOPC), phosphatidylserine (Sigma Chemical Co., No. P-7769), (PS), phosphatidylethanolamine (Sigma Chemical Co., No. P-4264), (PE), sphingomyelin (Sigma Chemical Co., No. S-7004), (Sph), and cholesterol (Wako Pure Chemical Ind., Ltd., No. 087-21), (Ch).

Potassium tetraphenylborate, $K^+ \cdot TPhB^-$, potassium dipicrylamide, $K^+ \cdot DPA^-$, and crystalviolet tetraphenylborate, $CV^+ \cdot TPhB^-$, were prepared according to the procedure described previously.[16] Magnesium salts of $TPhB^-$ and DPA^-, $Mg^{2+} \cdot (TPhB^-)_2$ and $Mg^{2+} \cdot (DPA^-)_2$, were synthesized by the methods proposed by Ueno et al.[17] Aqueous solutions containing sulfates of tetraphenylarsonium, $(TPhAs^+)_2 \cdot SO_4^{2-}$, tetrapentylammonium, $(TPenA^+)_2 \cdot SO_4^{2-}$, tetrabutylammonium, $(TBA^+)_2 \cdot SO_4^{2-}$, tetrapropylammonium, $(TPrA^+)_2 \cdot SO_4^{2-}$, tetraethylammonium, $(TEA^+)_2 \cdot SO_4^{2-}$, and tetramethylammonium, $(TMA^+)_2 \cdot SO_4^{2-}$, were obtained by titrating 0.05 M (mol dm^{-3}) chloride solutions of $TPhAs^+$, $TPenA^+$, TBA^+, $TPrA^+$, TEA^+, and TMA^+ with 0.05 M Ag_2SO_4 aqueous solution with the aid of a chloride ion selective electrode (a product of Horiba Co.) followed by the filtration of AgCl. An aqueous solution of magnesium picrate, $Mg^{2+} \cdot (Pic^-)_2$, was prepared by titrating 0.1 M solution of picric acid with a powder of $Mg(OH)_2$ and monitoring the pH of the solution. In order to get nitrobenzene solutions containing Mg^{2+} or SO_4^{2-}, 10 ml of nitrobenzene solution containing 10^{-3} M Bis(diphenylphosphiryl) ethane, (BDPPE), was shaken with 10 ml of aqueous solution containing 5×10^{-5} M $Mg^{2+} \cdot (DPA^-)_2$, $Mg^{2+} \cdot (Pic^-)_2$, or $(TPenA^+)_2 \cdot SO_4^{2-}$, respectively. BDPPE was obtained according to the procedure proposed by Chatt and Hart[18] and Umetani et al.[19,20]

The water used was purified by the triple distillations of deionized water. All other reagents were of reagent grade and were used without further purification.

Preparation of BLMs. The BLM used was obtained as a black lipid membrane by brushing decane solution of lipid(s) on the aperture of 1 mm in diameter created on a tetrafluoroethylene resin sheet of 0.2 mm thick (a product of Mitsui Fluorochemical Co.).[2,14] The decane solution was prepared dissolving 10 mg of a single lipid such as DOPC, PS, or PE, or 20 mg of an 1 : 1 mixture of lipids such as PC+Ch, DOPC+Ch, PS+Ch, PE+Ch, or Sph+Ch into 10 ml of decane. The formation of a BLM was confirmed by the microscopic observation of the area of the black lipid membrane and the capacitance measurement.[21]

Voltammetric Measurement. The BLM system employed in the present work is given in as Eq. 1.

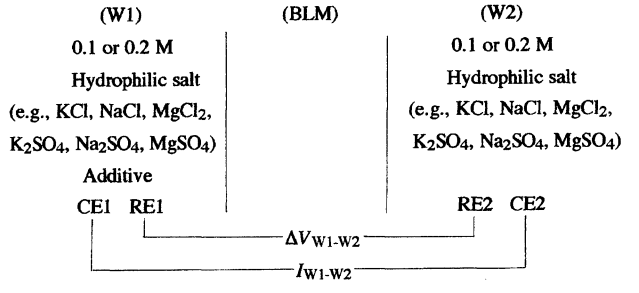

(1)

The electrolytic cell used for the voltammetric measurement with a BLM was essentially the same as that proposed by Tien.[2,14] It was placed in a Faraday cage during the measurement in order to decrease the noise generated by the environment. The voltammogram for the ion transfer from W1 and W2 through a BLM was recorded by scanning the potential difference between W1 to W2, ΔV_{W1-W2}, and by measuring the current between W1 and W2, I_{W1-W2}. Two silver–silver chloride electrodes, RE1 and RE2, and two platinum wire electrodes, CE1 and CE2, were used to apply ΔV_{W1-W2} and to measure I_{W1-W2}, respectively.

Voltammograms for the ion transfer through a liquid membrane, LM, and at the W/LM interfaces were recorded adopting the cell and the procedure described in previous papers.[13,15]

All voltammograms were measured by scanning ΔV_{W1-W2} at a rate of 0.01 $V\,s^{-1}$ at 25±0.5 °C unless otherwise mentioned. The potentiostat, function generator, and X–Y recorder used were identical with those used in the previous work.[13]

Results and Discussion

The Stability of the BLM Observed with and without Applying the Membrane Potential. BLMs composed of DOPC, PS, or PE were stable for more than 5 h after their formation in the cell of Eq. 1 with any hydrophilic salts, but BLMs of PC or Sph were unstable and difficult to form. The coexistence of Ch made all BLMs much more stable, and even BLMs of PC or Sph were stable for several hours when they were prepared from decane solution of 1 : 1 mixture of PC or Sph and Ch. Similar results were reported earlier.[2,22]

The BLMs once formed were broken down when the applied ΔV_{W1-W2} was scanned positively or negatively to certain voltages (breakdown voltages) which depended on the composition of the BLM and the species and concentration of the hydrophilic salt in aqueous phases. In this connection, when W1 and W2 contain sufficient concentration of electrolytes like in the present system (0.1 M), ΔV_{W1-W2} corresponds to the membrane potential as mentioned previously.[13] Table 1 summarizes mean breakdown voltages of various BLMs obtained by 10 repeated measurements with the cell system consisted of W1 and W2 containing 0.1 M $MgSO_4$. The addition of 10^{-6} M of a hydrophobic ion such as $TPhB^-$, DPA^-, CV^+, or $TPhAs^+$ made the absolute values of breakdown voltages larger in most cases as seen in Table 1, though the concentration of the additive was very low. The absolute values of breakdown voltages for all BLMs were rather smaller when 0.1 or 0.2 M KCl was employed in place of 0.1 M $MgSO_4$.

In the present work, potential ranges to observe voltammograms were chosen from Table 1 to be those where BLMs would never be broken.

Voltammograms for Transfer of Various Ions through a BLM Composed of PC and Ch. The voltammograms were investigated by employing a typical BLM made from decane containing a mixture of PC and Ch, and by choosing ions in aqueous phases in the light of standard Gibbs transfer free energy, $\Delta G^\circ_{tr,W\to Org}$, from aqueous, W, to organic, Org, such as nitrobenzene, NB, or 1,2-dichloroethane, DCE, which are summarized in Table 2.[23,24] Here, the $\Delta G^\circ_{tr,W\to Org}$ is presumed to be a good measure of the hydrophilic or hydrophobic property of an ion which determines

Table 1. Breakdown Voltages for Various BLMs with or without the Addition of a Hydrophobic Ion in One of Two Aqueous Phases Containing 0.1 M $MgSO_4$

BLM	Breakdown voltage (absolute value)/V				
	Ion added (10^{-6} M)				
	None	DPA^-	$TPhB^-$	CV^+	$TPhAs^+$
PC	—	—	—	—	—
DOPC	0.25	0.30	0.32	0.32	0.35
PS	0.12	0.17	0.18	0.18	0.18
PE	0.20	0.28	0.27	0.27	0.25
Sph	—	—	—	—	—
PC+Ch	0.13	0.20	0.20	0.27	0.20
DOPC+Ch	0.20	0.25	0.25	0.27	0.28
PS+Ch	0.15	0.18	0.20	0.20	0.21
PE+Ch	0.31	0.34	0.45	0.39	0.32
Sph+Ch	0.36	0.40	0.38	0.41	0.42

Table 2. Standard Gibbs Free Energies for Transfers, ΔG°_{tr}, of Various Ions from Aqueous, W, to Nitrobenzene, NB, or 1,2-Dichloroethane, DCE

Ion	W/NB	W/DCE	Category
	ΔG°_{tr}/kJ mol^{-1}	ΔG°_{tr}/kJ mol^{-1}	
DPA^-	−39.4		V
$TPhB^-$	−35.9	−35.1	IV
Pic^-	−4.6		III
ClO_4^-	8.0	17.2	II
Br^-	28.4	38.5	I
Cl^-	31.4	46.4	I
SO_4^{2-}	>67.3		I
EV^+	ca.−44[a)]		V
CV^+	−39.5		V
$TPhAs^+$	−35.9	−35.1	IV
$TPenA^+$	−35.1	−34.7	IV
TBA^+	−24.0	−21.8	IV
$TPrA^+$	−10.0	−8.8	III
TEA^+	−5.7	4.2	III
TMA^+	3.4	17.6	II
K^+	23.4		I
Na^+	34.2		I
Mg^{2+}	69.6		

a) S. Kihara and O. Shirai, unpublished work.

in the ion transport. In Table 2, ions are classified into five categories: i.e., hydrophilic ions with $\Delta G^\circ_{tr,W\to NB} \geq 10$ (kJ mol^{-1}; category I); slightly hydrophobic ions with $10 > \Delta G^\circ_{tr,W\to NB} \geq 0$ (kJ mol^{-1}; category II); rather hydrophobic ions with $0 > \Delta G^\circ_{tr,W\to NB} \geq -20$ (kJ mol^{-1}; category III); very hydrophobic ions with $-20 > \Delta G^\circ_{tr,W\to NB} \geq -37$ (kJ mol^{-1}; category IV); and extremely hydrophobic ions with $-37 > \Delta G^\circ_{tr,W\to NB}$ (kJ mol^{-1}; category V).

When an ion was added into one of two aqueous phases in the presence of a hydrophilic salt, the voltammogram was transformed depending on the property and concentration of the added ion.

The voltammograms observed can be classified into four types which will be denoted as Types **A**, **B**, **C**, and **D** hereafter.

Type A: Voltammograms observed with the cell in the absence of any extremely hydrophobic ion, very hydrophobic ion, or rather hydrophobic anion in aqueous phases.

In the voltammogram which was obtained with W1 and W2 containing a salt composed of hydrophilic ions (category I in Table 2), there was no peak indicative of the ion transfer. As an example, curve 1 in Fig. 1 gives the voltammogram recorded with W1 and W2 containing 0.1 M $MgSO_4$ by scanning ΔV_{W1-W2} in the region between +0.1 and −0.1 V and, simultaneously, by measuring I_{W1-W2}. Similar voltammograms without any peak were observed when the hydrophilic salt in W1 and W2 was NaCl, KCl, $MgCl_2$, K_2SO_4, or Na_2SO_4 instead of $MgSO_4$. The voltammograms of Type **A** were also observed when one of the slightly hydrophobic ions (category II) or rather hydrophobic cations (category III) was added in place of $MgSO_4$.

Type B: Voltammograms observed with the cell in the presence of an extremely hydrophobic anion, an extremely hydrophobic cation, or a very hydrophobic anion in W1 in

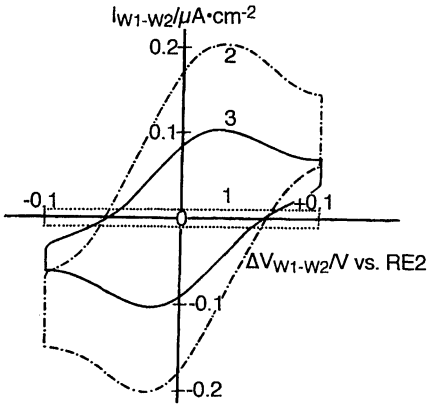

Fig. 1. Voltammograms for the ion transfer through a BLM composed of PC and Ch. Curve 1; 0.1 M $MgSO_4$ in both W1 and W2. Curves 2 and 3; as curve 1, but in the presence of 10^{-6} M DPA^- in W1 (curve 2) and 10^{-6} M $TPhB^-$ in W1 (curve 3).

addition to the hydrophilic salt.

In the voltammogram of Type **B** which was obtained by the addition of one of the extremely hydrophobic ions (category V) or very hydrophobic anions (category IV) into W1 of the system of Eq. 1 in the presence of a hydrophilic salt in W1 and W2, well established positive and negative peaks symmetrical about the origin (the point of 0 V and 0 A) appeared, even though the concentration of the added hydrophobic ion was very dilute; less than 10^{-6} M, and the ion was added into one of the two aqueous phases. The half-peak potentials of both the positive and negative peaks were around 0 V. An example of a voltammogram of Type **B** is shown as curve 2 in Fig. 1; this was observed when 10^{-6} M DPA^- was added as the form of $Mg^{2+}\cdot(DPA^-)_2$ into W1 of the BLM system in the presence of 0.1 M $MgSO_4$ in W1 and W2. The peak current density was nearly proportional to the concentration of DPA^- in the range between 5×10^{-8} and 10^{-5} M and to the square root of the scan rate of ΔV_{W1-W2} in the range between 0.01 and 0.1 V s^{-1}. It increased slightly with the increase of the concentration of the hydrophilic salt, $MgSO_4$, in aqueous phases from 0.1 to 1 M, and increased when the hydrophilic salt in aqueous phases was changed from 0.1 M $MgSO_4$ to 0.1 M K_2SO_4 or 0.1 M Na_2SO_4. Here, the current density was calculated by dividing the current observed by the area of the BLM measured microscopically.

Voltammograms observed by employing 0.1 M $MgCl_2$, 0.2 M KCl, or 0.2 M NaCl in place of 0.1 M $MgSO_4$, 0.1 M K_2SO_4, or 0.1 M Na_2SO_4, respectively, were almost identical with those with sulfates.

Adding $TPhB^-$ instead of DPA^- as the form of $Mg^{2+}\cdot(TPhB^-)_2$ into W1 of the system in the presence of 0.1 M $MgSO_4$ in W1 and W2, the voltammogram observed was that of Type **B** as shown as curve 3 in Fig. 1. The characteristics of the voltammogram were similar to those with DPA^-, except that the peak current density with $TPhB^-$ was smaller than that with DPA^-, even though the concentration of $TPhB^-$ was the same as that of DPA^-. Voltammograms with dilute $TPhB^-$ in W1 in the presence of 0.1 to 1 M $MgSO_4$, K_2SO_4, or Na_2SO_4 were identical with those in the presence of 0.1 to 1 M $MgCl_2$, KCl, or NaCl in W1 and W2, which was reported in the previous paper.[13]

The voltammograms of Type **B** were also observed by the addition of dilute (5×10^{-7} to 10^{-5} M) CV^+ or ethylviolet ion, EV^+, into one of two aqueous phases containing 0.1 M $MgSO_4$ or $MgBr_2$, respectively. The peak current density depended on the species of the anion in the hydrophilic salt, but was practically independent from the cation in the salt.

The characteristics of the peak currents with DPA^-, $TPhB^-$, or CV^+ are summarized in Table 3.

When an extremely hydrophobic ion or very hydrophobic anion was added into both aqueous phases in the same concentration, the positive and negative peaks symmetrical about the origin were larger compared with those observed when the ion was added only to W1 (e.g., about 1.6 times when the added ion was 10^{-6} M DPA^- and the hydrophilic salt was 0.1 M $MgSO_4$).

Type C: Voltammograms observed with the cell in the presence of a very hydrophobic cation in W1 in addition to the hydrophilic salt.

In the voltammogram of Type **C** which was obtained by the addition of one of the very hydrophobic cations (category IV) such as $TPenA^+$, TBA^+, or $TPhAs^+$ in 10^{-5} to 10^{-4} M concentration into W1 of the system in the presence of 0.1 to 1 M hydrophilic salt such as $MgSO_4$, K_2SO_4, or Na_2SO_4 in W1 and W2, a positive and a negative current of different magnitudes appeared around the origin.

Curve 1 in Fig. 2 is a typical example of Type **C** observed with 10^{-4} M $TPenA^+$ in W1 and 0.1 M $MgSO_4$ in both W1 and W2. The magnitudes of the positive and negative peaks (or limiting currents) were proportional to the concentration of the very hydrophobic ion added in the range between 10^{-5} and 10^{-4} M, while the ratio of the positive to negative peak (or limiting current) was almost constant. The ratio depended on the kind of the hydrophobic cation added. Among cations which belong to category IV in Table 2, the more hydrophobic ion gave the smaller ratio.

The characteristics of peaks or currents of Type **C** are

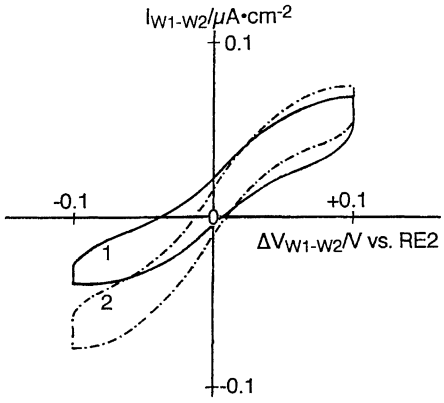

Fig. 2. Voltammograms for the ion transfer through a BLM composed of PC and Ch. Curve 1; 10^{-4} M $TPenA^+$ in W1 and 0.1 M $MgSO_4$ in both W1 and W2. Curve 2; as curve 1, but in the presence of 10^{-4} M $TPenA^+$ in W1 and W2.

Table 3. Peak Currents in Voltammograms of Type **B** Observed with the BLM Composed of PC+Ch

Supporting electrolyte in W1 and W2	Peak current density / μA cm^{-2}		
	Ion added in W1 (10^{-6} M)		
	DPA^-	$TPhB^-$	CV^+
0.1 M $MgSO_4$	0.20±0.03	0.10±0.02	0.04±0.01
1 M $MgSO_4$	0.23±0.03	0.12±0.02	0.05±0.01
0.1 M K_2SO_4	0.60±0.10	0.25±0.03	0.04±0.01
0.1 M Na_2SO_4	0.22±0.03	0.12±0.02	0.04±0.01
0.1 M $MgBr_2$	0.21±0.03	0.12±0.02	0.05±0.01
0.1 M $MgCl_2$	0.20±0.03	0.11±0.02	ca.0
0.2 M KCl	0.62±0.10	0.23±0.03	ca.0
0.2 M NaCl	0.19±0.03	0.13±0.02	ca.0

Table 4. Currents at ΔV_{W1-W2}=+0.1 and −0.1 V, $I(+)$ and $I(-)$, Observed in Voltammograms of Type **C** with W1 and W2 Containing 0.1 M of Various Magnesium Salt

Salt in W1 and W2	Current density / μA cm^{-2}					
	Ion added in W1 (10^{-5} M)					
	$TPhAs^+$		$TPenA^+$		TBA^+	
	$I(+)$	$I(-)$	$I(+)$	$I(-)$	$I(+)$	$I(-)$
0.1 M $MgSO_4$	0.09±0.02	−0.05±0.01	0.04±0.01	−0.02±0.01	0.03±0.01	−0.01±0.005
0.1 M $MgBr_2$	0.15±0.03	−0.11±0.02	0.06±0.02	−0.03±0.01	0.04±0.01	−0.02±0.01
0.1 M $MgCl_2$	ca.0	ca.0	ca.0	ca.0	ca.0	ca.0

summarized in Table 4.

When the very hydrophobic cation was added into both aqueous phases at the same concentration, the positive and the negative peaks or currents were the same magnitude and symmetrical about the origin. Curve 2 in Fig. 2 is the example which was recorded by adding 10^{-4} M $TPenA^+$ and 0.1 M $MgSO_4$ in both W1 and W2.

Type D: Voltammogram observed with the cell in the presence of a rather hydrophobic anion in W1 in addition to the hydrophilic salt.

In the voltammogram of Type **D** which was observed by the addition of a rather hydrophobic anion (category III) in fairly high concentrations such as 10^{-4} to 10^{-3} M into W1 of the BLM system with W1 and W2 containing a hydrophilic salt, a current decrease, which resembles the current limiting the potential window (so-called the final descent), and a small limiting current appear. Curve 1 in Fig. 3 is a typical example observed with 10^{-4} M Pic^- in W1 and 0.1 M $MgSO_4$ in both W1 and W2. Current densities at ΔV_{W1-W2}=−0.1 (the final descent) and +0.1 V (the limiting current) depended on the concentrations of both Pic^- and Mg^{2+} in W1, as summarized in Table 5.

In this connection, the negative current (the final descent) might reach a limiting value if a wide ΔV_{W1-W2} could be applied, though it was not realized with the BLM composed of PC+Ch because the breakdown potential of the BLM was not wide enough. Actually, the limiting current was observed with the BLM of PE+Ch, which is more stable than that of PC+Ch.

When Pic^- was added into both aqueous phases at the same concentrations, the final rise and the final descent which were symmetrical about the origin were observed, as shown as curve 2 in Fig. 3.

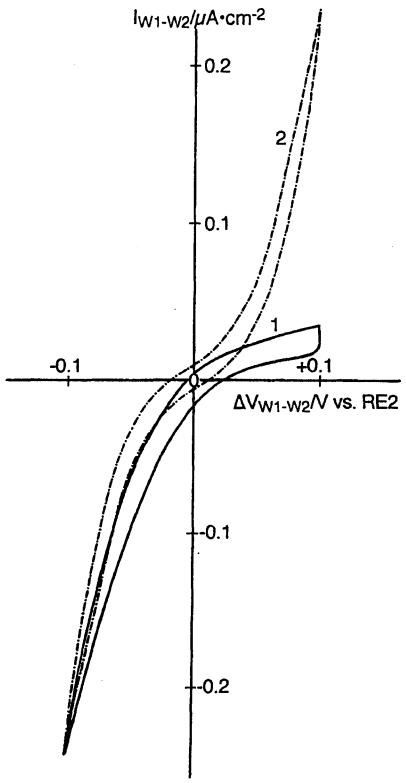

Fig. 3. Voltammograms for the ion transfer through a BLM composed of PC and Ch. Curve 1; 10^{-3} M Pic^- in W1 and 0.1 M $MgSO_4$ in both W1 and W2. Curve 2; as curve 1, but in the presence of 10^{-3} M Pic^- in W1 and W2.

Ion Transfer Processes Involved in Voltammograms

Table 5. Currents at ΔV_{W1-W2}=+0.1 and −0.1 V, Observed in Voltammograms of Type **D** by the Addition of Pic^- into W1 in the Presence of 0.1 or 0.5 M $MgSO_4$ in W1 and W2

Concn of Pic^- in W1	Concn of $MgSO_4$ in W1 and W2	Current density / $\mu A\,cm^{-2}$	
		ΔV_{W1-W2}=−0.1 V (Final descent)	ΔV_{W1-W2}=+0.1 V (Limiting current)
10^{-4} M	0.1 M	−0.25	0.03
10^{-3} M	0.1 M	−1.90	0.40
10^{-4} M	0.5 M	−0.29	0.09

through BLMs. In the previous paper,[13] the voltammogram for the transfer of an ion from W1 to W2 through an LM was analyzed by taking into account the ion transfer processes at the W1/LM and LM/W2 interfaces and the mass transfer in the membrane. The voltammogram through a BLM was also investigated and compared with that through an LM. The ion transport process through a BLM was analogous to that through an LM, though the BLM was much thinner than the LM.

In the following, the ion transport processes involved in the voltammograms through BLMs obtained in the present work will be elucidated by using methods and concepts analogous to those proposed in the previous work.[13]

Curves 1 in Figs. 4, 5, 6, and 7 are voltammograms for ion transfers through LMs, VITTM, observed with LM systems as Eqs. 2, 3, 4, and 5, respectively, by scanning ΔV_{W1-W2} and measuring I_{W1-W2}.

(W1)	(NB-LM)	(W2)	
0.1 M $MgSO_4$	10^{-3} M BDPPE, 0.1 M CV^+•$TPhB^-$	0.1 M $MgSO_4$	
as Eq. (2) + 5×10^{-7} M Mg^{2+}•$(DPA^-)_2$	as Eq. (2) + 5×10^{-5} M Mg^{2+}•$(DPA^-)_2$	as Eq. (2)	(2)
as Eq. (2) + 5×10^{-5} M $(TPenA^+)_2$•SO_4^{2-}	as Eq. (2) + 5×10^{-5} M $(TPenA^+)_2$•SO_4^{2-}	as Eq. (2)	(3)
as Eq. (2) + 5×10^{-4} M Mg^{2+}•$(Pic^-)_2$	as Eq. (2) + 5×10^{-5} M Mg^{2+}•$(Pic^-)_2$	as Eq. (2)	(4)
CE1 RE1	RE3 RE4	RE2 CE2	(5)

$\Delta V_{W1/LM}$ $\Delta V_{LM/W2}$ ΔV_{W1-W2} I_{W1-W2}

The LM consisted of NB into which CV^+·$TPhB^-$ and BDPPE were added as a supporting electrolyte and a neutral ligand to stabilize Mg^{2+} in the LM and to facilitate the transfer of Mg^{2+} from W1 and W2 to LM.[25] The supporting electrolyte in aqueous phases was 0.1 M $MgSO_4$. Potential differences at the W1/LM and LM/W2 interfaces, $\Delta V_{W1/LM}$ and $\Delta V_{LM/W2}$, were measured as the potential of RE1 vs. RE3 and that of RE4 vs. RE2, respectively. Here, RE3 and RE4 were $TPhB^-$ ion selective electrodes[16] placed in LM near the interfaces.

Curves 2 and 3 in Figs. 4, 5, 6, and 7 are voltammograms for the ion transfer at the W1/LM and LM/W2 interfaces, respectively, recorded by monitoring variations of $\Delta V_{W1/LM}$ and $\Delta V_{LM/W2}$ as the function of I_{W1-W2} during the measurements of VITTMs.

Ion transfer reactions involved in voltammetric waves at the W1/LM and LM/W2 interfaces (curves 2 and 3 in Figs. 4, 5, 6, and 7) were assigned to those indicated in Figs. 4, 5, 6, and 7 by consulting with voltammetric results on the ion transfer at the aqueous/nitrobenzene interface, which were obtained by changing concentrations of ions in W1, LM, or W2 (cf. Ref. 13).

According to the results on the VITTM reported in the previous paper,[13] the relation of Eq. 6 holds among ΔV_{W1-W2}, $\Delta V_{W1/LM}$, and $\Delta V_{LM/W2}$ in curves 1, 2, and 3, respectively, regardless of the magnitude of I_{W1-W2}.

$$\Delta V_{W1-W2} = \Delta V_{W1/LM} + \Delta V_{LM/W2} + I_{W1-W2}R. \quad (6)$$

Here, R means the sum of the resistances in aqueous phases and membrane phases. When W1, LM, and W2 contain sufficient concentraitons of electrolytes as in the present systems, the contribution of $I_{W1-W2}R$ to ΔV_{W1-W2} is not significant, and the 3rd term in the right hand side of Eq. 6 can be neglected. The relation of Eq. 6 suggests that the membrane potential in the presence of sufficient electrolytes in each phase of the membrane system is primarily determined by the potential differences at two interfaces, which depend on ion transfer reactions at the interfaces.

Taking into account ion transfer reactions at the W1/LM and LM/W2 interfaces and the relation of Eq. 6 in a similar manner to that in the previous paper,[13] the final rise in the VITTM (curve 1) in Fig. 4 is considered to be composed of the transfer of Mg^{2+} from W1 to LM (the final rise in curve 2) and those of SO_4^{2-} from W2 to LM and CV^+ from LM to W2 (the final rise in curve 3). The final descent in the VITTM is attributable to transfers composed of the transfer of Mg^{2+} from W2 to LM (the final descent in curve 3) and those of SO_4^{2-} from W1 to LM and CV^+ from LM to W1 (the final descent in curve 2).

Transfer reactions responsible for VITTMs (curves 1) in Figs. 5, 6, and 7 are estimated as those indicated in these figures.

Each VITTM observed with the LM shows the following characteristics:

VITTM (curve 1) in Fig. 4. Since highly hydrophilic Mg^{2+} and SO_4^{2-} are not easily transferred from W to

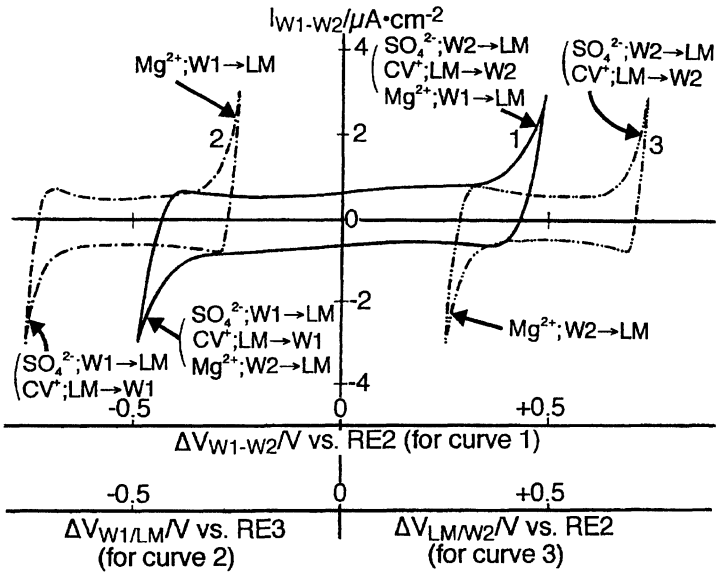

Fig. 4. Voltammograms for the ion transfer through an LM (curve 1), at the W1/LM interface (curve 2) and at the LM/W2 interface (curve 3). Compositions of W1, LM and W2; 0.1 M $MgSO_4$ in W1, 10^{-3} M BDPPE+0.1 M CV^+·$TPhB^-$ in LM, 0.1 M $MgSO_4$ in W2.

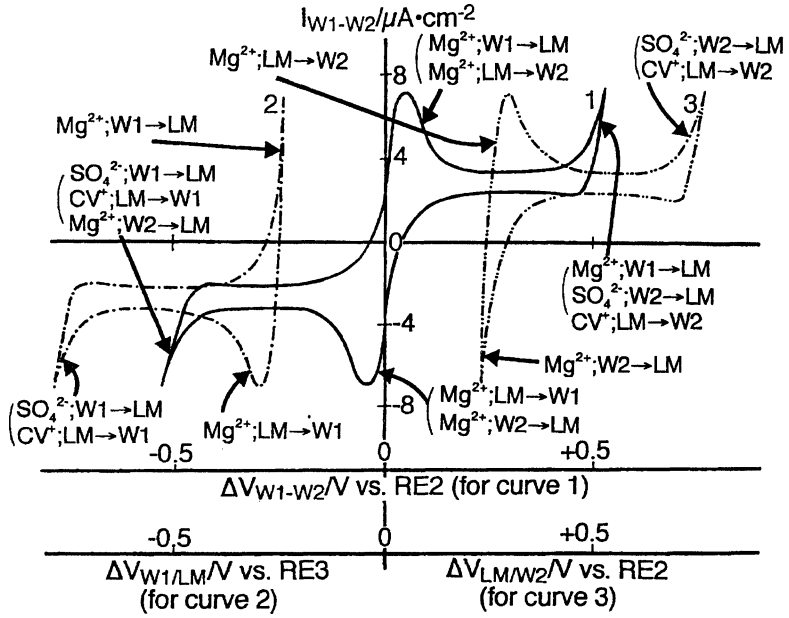

Fig. 5. Voltammograms the same as those in Fig. 4, but in the presence of 5×10^{-7} M Mg^{2+}·$(DPA^-)_2$ in W1 and 5×10^{-5} M Mg^{2+}·$(DPA^-)_2$ in LM.

LM and highly hydrophobic CV^+ and $TPhB^-$ are not easily transferred from LM to W even in the presence of BDPPE in the LM, a wide polarized region (potential window) is observed.

VITTM (curve 1) in Fig. 5. Since DPA^- is too hydrophobic to transfer from LM to W within the potential window, the transfer of DPA^- from LM to W1 and that from LM to W2 are not observed. Since the concentration of DPA^- in W1 is very low, the transfer of DPA^- from W1 to LM is not observed.

VITTM (curve 1) in Fig. 6. Since the positive current peak is due to the composite transfers of $TPenA^+$ from W1 to LM, SO_4^{2-} from LM to W1, CV^+ from W1 to LM, SO_4^{2-} from W2 to LM, and CV^+ from LM to W2, the peak height of the negative current due to the composite transfers of SO_4^{2-} from W1 to LM, CV^+ from LM to W1, CV^+ from W2 to LM, and SO_4^{2-} from LM to W2 is a half of that of the positive current.

VITTM (curve 1) in Fig. 7. Since Mg^{2+}·$(Pic^-)_2$ is added in W1 in a fairly high concentration (e.g., 5×10^{-4} M) and in LM in a concentration less than that in W1 (e.g., 5×10^{-5} M) as Eq. 5, a fairly large negative current peak and a positive limiting current of which magnitude is less than the negative peak (about 1/10) appear at potentials apart from the origin in the VITTM.

The shapes of curves 1 in Figs. 4, 5, 6, and 7 in the po-

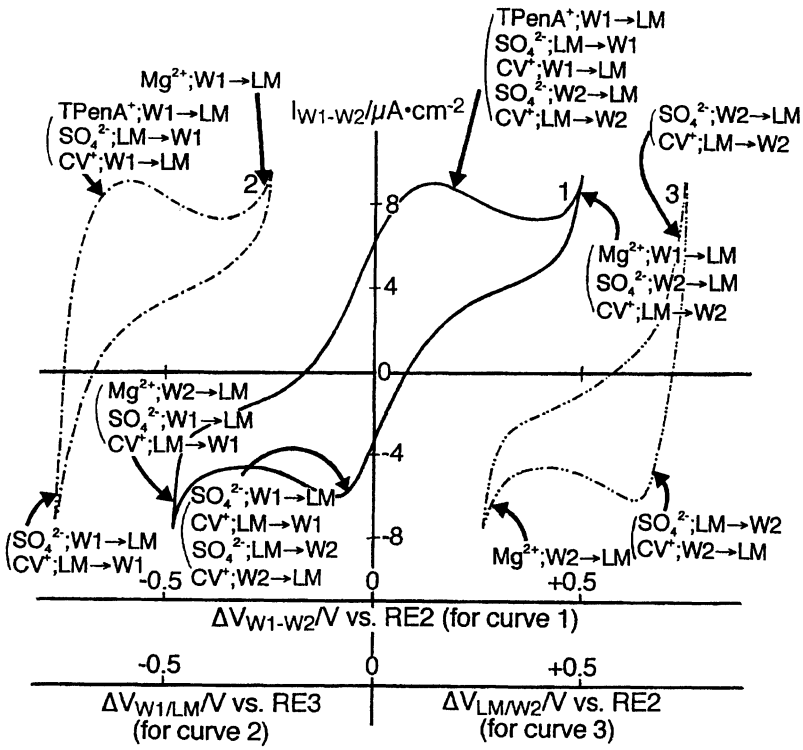

Fig. 6. Voltammograms the same as those in Fig. 4, but in the presence of 5×10^{-5} M $(TPenA^+)_2\cdot SO_4^{2-}$ in W1 and 5×10^{-5} M $(TPenA^+)_2\cdot SO_4^{2-}$ in LM.

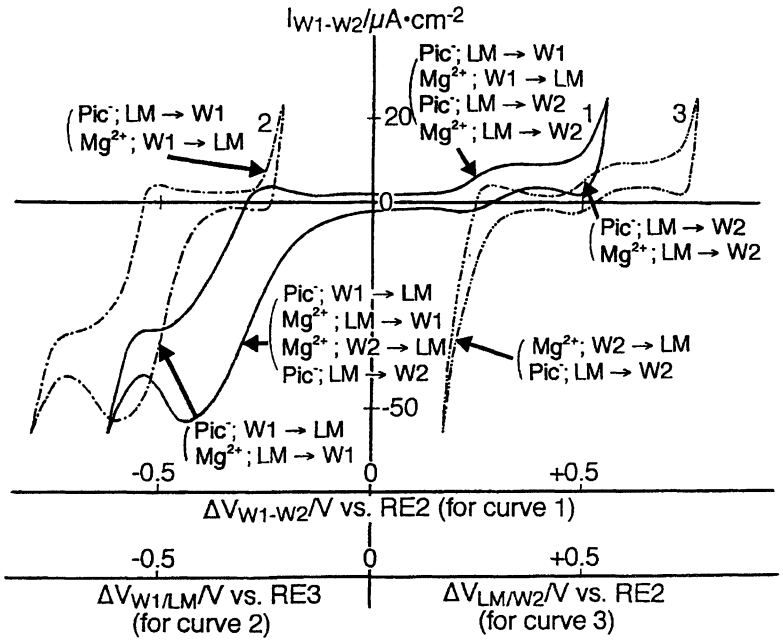

Fig. 7. Voltammograms the same as those in Fig. 4, but in the presence of 5×10^{-4} M $Mg^{2+}\cdot(Pic^-)_2$ in W1 and 5×10^{-5} M $Mg^{2+}\cdot(Pic^-)_2$ in LM.

tential region between +0.1 and −0.1 V resemble those of voltammograms of Types **A**, **B**, **C**, and **D** (curves 1 and 2 in Fig. 1, curves 1 in Figs. 2 and 3), respectively, observed with the BLM. Therefore, it may be natural to consider that the processes of ion transfers through BLMs are analogous to those through LMs. Taking into account that BLM systems do not contain $CV^+\cdot TPhB^-$, ion transfer reactions responsible to voltammograms of Types **A** to **D** were assigned as follows;

Type A: Few ions composing the hydrophilic salt in aqueous phases transfer to the hydrophobic BLM. Therefore, the ionic current flow through the BLM is negligible when the applied membrane potential is not very large, such as between +0.1 and −0.1 V. In this case, the contribution

of the ohmic drop [$I_{W1-W2}R$ in Eq. 6] on ΔV_{W1-W2} should also be taken into account, since the BLM contains little electrolyte and the resistance of the BLM is large.

Type B: The VITTM of this type was observed when one of the extremely hydrophobic ions or very hydrophobic anions was added in W1. In this case, the hydrophobic ion (e.g., DPA^-) may easily be accumulated by the spontaneous distribution into the hydrophobic BLM. The distribution should be accompanied by the transfer of the hydrophilic ion (e.g., Mg^{2+}) as the counter ion of the hydrophobic ion in order to hold electroneutrality in both W1 and BLM. If we accept this assumption, the BLM system for Type **B** is analogous to the LM system of Eq. 3, and hence the transfer reactions involved in the VITTM of this type can be considered to be identical with those for the VITTM in Fig. 5. The positive current peak is due to the transfer of Mg^{2+} from W1 to BLM and that of Mg^{2+} from BLM to W2, and the negative current peak due to the transfer of Mg^{2+} from W2 to BLM and that of Mg^{2+} from BLM to W1.

The ion transfer through a BLM of Type **B** has been investigated voltammetrically by several authors.[8,12,26—29] All of these authors assumed the transfer of the hydrophobic ion such as $TPhB^-$ or DPA^- in their explanations of the current peaks in the VITTM. On the other hand, based on the above described analysis of the VITTM, we consider that hydrophilic ion which has been concentrated in the BLM with the aid of the hydrophobic ion transfers from the BLM to W2 (or W1), and, simultaneously, the same amount of the hydrophilic ion in W1 (or W2) transfers to the BLM. During the transfer of the hydrophilic ion, the hydrophobic ion concentrated in the BLM remains there, behaving like a mobile site for the hydrophilic ion. Consequently, the concentration of the hydrophilic ion in the BLM maintains at constant. Adopting the mechanism presented here, the characteristics of the positive and negative current peaks in the VITTM such as ΔV_{W1-W2} where peaks appear, the mutually symmetrical peaks, the extraordinary large current peaks, and the dependence of magnitudes of peaks on the kind or concentration of the hydrophilic ions in aqueous phases can be understood easily. Also the potential difference between two peaks and its dependence on the scan-rate of ΔV_{W1-W2} can be understood, as will be discussed later.

Type C: The hydrophobicity of the added ion in W1 for this type is a little weaker than that for Type **B**. Hence, the addition of the ion to be a concentration higher than that in the case of Type **B** is required to concentrate the added ion into the BLM at a concentration identical with that of the ion in the BLM for Type **B**. When a proper concentration (e.g., 5×10^{-4} M) of the ion (e.g., $TPenA^+$) is condensed spontaneously in the BLM together with the hydrophilic counter ion (e.g., SO_4^{2-}), the BLM system for Type **C** is analogous to the LM system of Eq. 4, and hence the transfer reactions involved in the VITTM of this type are analogous to those in Fig. 6. Therefore, it is concluded that the positive current peak of the VITTM is composed of the transfer of $TPenA^+$ from W1 to BLM, that of SO_4^{2-} from BLM to W1, and that of SO_4^{2-} from W2 to BLM, and the negative current peak of the VITTM the transfer of SO_4^{2-} from W1 to BLM and that of SO_4^{2-} from BLM to W2. Since the current due to the transfer of SO_4^{2-} from BLM to W1 is equal to that of SO_4^{2-} from BLM to W2, the magnitude of the positive current density, $I(+)$, which includes the current due to the transfer of $TPenA^+$ from W1 to BLM in addition to the current due to the transfer of SO_4^{2-} from BLM to W1, is larger than that of the negative current density, $I(-)$, which is caused by the transfer of SO_4^{2-} from BLM to W2 alone.

When Br^-, which is more hydrophobic than SO_4^{2-}, is used instead of SO_4^{2-} in the BLM system of Eq. 4, the concentration of Br^- distributed into the BLM is expected to be larger than that of SO_4^{2-}. Hence, the currents due to the transfer of Br^- from BLM to W1 and that from BLM to W2 may be larger than those observed with SO_4^{2-}. This consideration may explain the result in Table 4 that $I(+)$ caused by both the transfer of Br^- from BLM to W1 and that of $TPenA^+$ from W1 to BLM and $I(-)$ caused by the transfer of Br^- from BLM to W2 are larger, and the ratio of $I(+)$ to $I(-)$ is smaller and closer to unity than those observed with SO_4^{2-}. Here, the current due to the transfer of $TPenA^+$ is considered to be unchanged by the use of Br^- instead of SO_4^{2-}.

When Cl^- was used instead of SO_4^{2-}, $I(+)$ and $I(-)$ were nearly zero and the VITTM was of Type **A**, which means that not much Cl^- is transferred between W1 and W2 through a BLM in accordance with the work on the anion permeation across BLMs.[30] This result indicates that the distribution of Cl^- to the BLM is less than that of SO_4^{2-}, even though Cl^- is more hydrophobic than SO_4^{2-}. Though further investigation is required, we think that specific interaction between SO_4^{2-} and the component of the BLM is responsible for the result.

Type D: The added anion in W1 for this type is not very hydrophobic. Hence, the ion is not concentrated into the BLM at a concentration identical with that of the ion in the BLM for Type **B** or **C** unless a rather high concentration of the ion is added to W1. When a proper concentration (e.g., 5×10^{-4} M) of the ion is condensed spontaneously into the BLM together with the hydrophilic counter ion (e.g., Mg^{2+}), the BLM system for Type **D** is analogous to the LM system of Eq. 5. Hence, the transfer reactions involved in the VITTM of this type are considered to be identical with those for the VITTM in Fig. 7. The positive limiting current is due to the transfer of Pic^- from BLM to W1, that of Mg^{2+} from W1 to BLM, that of Pic^- from BLM to W2, and that of Mg^{2+} from BLM to W2, and the negative current which looks like the final descent is due to the transfer of Pic^- from W1 to BLM, that of Mg^{2+} from BLM to W1, that of Pic^- from BLM to W2, and that of Mg^{2+} from W2 to BLM. Here, the negative current is attributable to a part of a negative current peak such as that in curve 3 in Fig. 7 which might be observed if ΔV_{W1-W2} could be scanned to a more negative value than -0.1 V. This could not be attained here because of the breakdown of the BLM.

In order to make the above described similarity of the ion transfer process through BLM to that through the LM convincing, the mass transfer in the BLM should be comparable

to that in the LM. It has been often believed based on the permeation coefficient, P, that a hydrophilic ion transfers through a BLM only with difficulty, though a hydrophobic ion transfers easily.[5,6] However, this argument does not necessarily mean that the mass transport (diffusion) of the hydrophilic ion in the BLM is very slow. Taking into account the fact that P is composed of diffusion coefficient of the ion, D, distribution coefficient of the ion between W and BLM, K_d, and the thickness of the BLM, d,[31,32]

$$P = K_d D/d, \tag{7}$$

the main reason for the low transferability (small P) of a hydrophilic ion through a BLM is attributable to the low distribution (small K_d) from W to the BLM. The mass transport of the hydrophilic ion once distributed into the BLM with the aid of a hydrophobic ion, which is assumed in the explanation of VITTM of Types **B**, **C**, and **D** in the present paper, is considered to be faster than a hydrophobic ion since the size of hydrophilic ion is much smaller than hydrophobic ions (cf., Einstein–Stokes Eq. for D[33]). In fact, Hauser et al. reported D of Na^+ in a BLM composed of phosphatidylcholine as 1.1×10^{-7} cm^2 s^{-1} based on a radio isotope technique.[34] This D is comparable to D of DPA^- in BLMs (1×10^{-7}cm^2 s^{-1}[35]) but smaller than D of Na^+ in NB (1×10^{-6} cm^2 s^{-1}).

The Ion Transfers through BLMs Composed of Various Lipids. As described above, the peak height of the voltammogram of Type **B** is controlled by the concentration of the hydrophilic ion in a BLM which has been distributed spontaneously into the BLM as the counter ion of the hydrophobic ion. The distribution of the added ion with the counter ion is determined by ΔG_{tr} of these ions from the aqueous to the BLM which may depend on the interaction between the distributed ions and lipid(s) composing the BLM.

Table 6 summarizes peak current densities observed in voltammograms recorded with the cell system of Eq. 1 equipped with BLMs of different compositions. In this investigation, a hydrophobic ion such as EV^+, CV^+, $TPhAs^+$, DPA^-, or $TPhB^-$ was added in 10^{-6} M concentration into one of two aqueous phases containing 0.1 M $MgSO_4$. The indication of **C** or **D** in the table means that the peak of Type **B** was not observed when the hydrophobic ion was 10^{-6} M but the current of Type **C** or **D** appeared when the concentration of the hydrophobic ion was increased to be 10^{-4} M or more.

The followings can be read from Table 6: (i) In accordance with the results summarized by Flewelling and Hubbell,[36] the peak current density was larger when the more hydrophobic one between two cations (CV^+ or EV^+) or between two anions ($TPhB^-$ or DPA^-) was adopted as the additive irrespective of the composition of the BLM. (ii) The peak current density with $TPhB^-$ or DPA^- was larger than that with $TPhAs^+$ or CV^+, respectively, though the hydrophobicity of $TPhB^-$ or DPA^- are almost identical with that of $TPhAs^+$ or CV^+ (cf. ΔG°_{tr} in Table 2), respectively, suggesting that hydrophobic anions are distributed into most of BLMs more easily than hydrophobic cations of hydrophobicities similar to the anions. (iii) The peak current density with $TPhB^-$ or DPA^- increased and that with CV^+ decreased when BLM composed of DOPC+Ch or PE+Ch was used instead of BLM composed of DOPC or PE, respectively. When BLM of PS+Ch was used instead of BLM of PS, peak current densities with all of hydrophobic ions ($TPhB^-$, DPA^-, $TPhAs^+$, CV^+, or EV^+) increased.

The variation of the current density, which is strongly related to the condensation of the added ion into a BLM, with various BLMs of different lipids has been discussed by several authors.[37,38]

Reviewing these works, we find that all of authors assumed the positive potential in the BLM near to the W/BLM interface or in the bulk of the BLM which is induced by functional groups oriented at the interface. They explained the preferable condensation of hydrophobic anion based on the interaction between the hydrophobic ion distributed in the BLM and the positive potential inside the BLM. However, no attention has been paid to the hydrophilic ion which moved into the BLM as a counter ion of the hydrophobic ion. Adopting their explanations, it is difficult to understand not only the dependence of the peak current density on the kind or concentration of the hydrophilic ion in W1 or W2, but also the ion transfer reaction which must occur at the W/BLM interface other than where the transfer of the hydrophobic ion proceeds in order to hold the electroneutrality in aqueous and membrane phases.

Distinct from previous authors, the role of the hydrophilic ion which distributes in the BLM as the counter ion of the hydrophobic ion has been found in the present work to be important to explain the ion transfer reaction through the BLM as well as the condensation of both the hydrophilic and hydrophobic ions into the BLM. Especially when the ion transfer is of Type **B**, the current flowing through the BLM is carried mostly by the hydrophilic ion (when Type **C** or **D**, the hydrophobic ion participates in the transfer in addition to the hydrophilic ion). In this connection, if the BLM is regarded as an organic phase, Org, the following relation proposed for the ion-pair extraction may be a good guide to understand the distribution of an ion into a BLM together with a counter ion. Equation 8 holds between distribution ratios, D_M and D_X, of a cation, M^+, and an anion, X^-, and standard Gibbs transfer free energies of M^+ and X^- from W to Org, when W containing a salt, $M^+\cdot X^-$, is equilibrated with an equivolume of Org.[39]

$$\ln D_M = \ln D_X = -(\Delta G^\circ_{tr,M} + \Delta G^\circ_{tr,M})/2RT \tag{8}$$

Here, Eq. 8 was derived by neglecting ion-pair formations in both W and Org.

Based on the present work,[13] the characteristics (i) to (iii) observed in VITTMs with various BLMs can be explained as follows: (i) Since not only the distribution ratio of the hydrophobic ion from W to BLM but also that of the hydrophilic ion are estimated to be larger when a hydrophobic ion of smaller ΔG°_{tr} is added to W in the presence of hydrophilic ion, peaks in VITTM of Type **B** which depend on

Table 6. Peak Currents in Voltammograms Observed with BLMs of Various Compositions W1 Contained 0.1 M $MgSO_4$ and 10^{-6} M of an Additive.

Lipid composing BLM	Peak current density / μA cm^{-2}				
	Ion added in W1 (10^{-6} M)				
	DPA^-	$TPhB^-$	EV^+	CV^+	$TPhAs^+$
DOPC	0.40±0.05	0.10±0.01	0.12±0.03	0.07±0.02	(C)
PS	0.20±0.02	0.10±0.01	0.11±0.02	0.06±0.01	(C)
PE	0.09±0.01	(D)	(C)	(D)	(D)
DOPC+Ch	0.50±0.10	0.14±0.02	0.09±0.02	0.05±0.01	(C)
PC+Ch	0.20±0.03	0.10±0.02	0.07±0.02	0.04±0.01	(C)
PS+Ch	0.09±0.01	(D)	0.25±0.04	0.15±0.02	(C)
PE+Ch	0.15±0.03	0.06±0.01	(C)	(D)	(D)
Sph+Ch	0.18±0.03	0.07±0.01	(C)	(D)	(D)

the concentration of hydrophilic ion in the BLM are larger when a more hydrophobic ion (with smaller ΔG_{tr}°) is added to W1. (ii) The short-range interaction (complex formation) between hydrophilic ions such as Mg^{2+}, Na^+, K^+, SO_4^{2-}, or Cl^- and functional groups, –OH or –C=O, in lipids composing BLMs is expected from the comparison of ΔG_{tr}° of hydrophilic ions from W to various alcohols with those from W to NB or DCE in the absence of the functional groups.[40,41] Since the interaction for hydrophilic cations which distribute into BLM as the counter ions of hydrophobic anions is larger than that for hydrophilic anions which distribute into BLM with hydrophobic cations, the concentration of hydrophilic cation (and hence hydrophobic anion) in BLM is larger than that of hydrophilic anion (and hence hydrophobic cation). This explains the reason why the peak in the VITTM of Type **B** is larger when a hydrophobic anion is added into W1 of the BLM system than when a hydrophobic cation is added, even though the hydrophobicity of the hydrophobic anion is identical with that of the hydrophobic cation. (iii) One reason for the increase of the peak by the coexistence of Ch in a BLM is considered to be the stabilization of hydrophilic ions through the short-range interaction with –OH [cf., (ii)] of which concentration in BLM increases by the coexistence of Ch. Another reason may be the structural change of BLM caused by the coexistence of Ch which may be remarkable especially for the BLM composed of PE. The BLM of PE is reported to be highly structured,[42,43] and hence it requires more energy to form a cavity to immerse a bulky ion in the BLM than other weakly-structured BLM. This means that the distribution of a hydrophobic ion and its counter ion (hydrophilic ion) into the BLM of PE is smaller than that into other BLM. When Ch coexists with the BLM of PE, the structure of the BLM is weakened and the distributions of a hydrophobic ion and its counter ion become larger. Therefore, larger peaks were observed in the VITTM of Type **B** with the BLM in the presence of Ch. The effect of Ch observed when a hydrophobic cation (CV^+ or EV^+) or a hydrophobic anion ($TPhB^-$ or DPA^-) was added to the system equipped with BLM of DOPC or PS, respectively, can not be understood by the above-described explanation, and requires further consideration.

Effect of Concentration of the Additive or Scan-Rate of Membrane Potential on the Peak Potential. The peak potentials observed in the VITTM of Type **B** shifted, and hence the potential difference between the positive and negative peaks varied, when the peak currents were altered by changing the concentration of the additive in W1 or the scan-rate of ΔV_{W1-W2}. e.g., Potentials of positive peaks observed with the cell of Eq. 1 in the presence of DPA^- in W1 were 0.040, 0.043, 0.046, and 0.055 V when concentrations of DPA^- were 5×10^{-7}, 10^{-6}, 2×10^{-6}, and 5×10^{-6} M, respectively. The potentials with the cell in the presence of 10^{-6} M DPA^- were 0.043, 0.044, 0.047, 0.049, and 0.053 V when scan-rates of ΔV_{W1-W2} were 0.01, 0.02, 0.05, 0.10, and 0.20 V s^{-1}, respectively.

Similarly to the result observed with the BLM system, the peak potentials in the VITTM observed with the LM system of Eq. 3 shifted when the concentration of $Mg^{2+}\cdot(DPA^-)_2$ in the LM or the scan-rate of ΔV_{W1-W2} was changed. However, the peak potentials in voltammograms at the W1/LM and LM/W2 interfaces which were recorded simultaneously with the VITTM were independent of the concentration or the scan-rate indicating that the ion transfer reactions at these interfaces were controlled by the diffusion of Mg^{2+} in the LM (i.e., reversible).

The shift of peak potential in the VITTM observed with the LM can be explained on the basis of Eq. 6 as follows. In this discussion, the positive peak in curve 1 (VITTM) in Fig. 5 is taken as an example. The peak appears due to the composite transfer of Mg^{2+} from W1 to LM which is observed as the final rise in the voltammogram at the W1/LM interface (see, curve 2 in Fig. 5) and that Mg^{2+} from LM to W2 which is observed as a peak in the voltammogram at the LM/W2 interface (see, curve 3 in Fig. 5). When the concentration of Mg^{2+} in LM or the scan-rate of ΔV_{W1-W2} is increased, the peak current increases though the peak potential in curve 3 remains at a definite $\Delta V_{LM/W2}$. Since magnitudes of currents at two interfaces should be the same in a membrane system, when the peak current at the LM/W2 interface increases, the corresponding current at the W1/LM interface increases along the slope of the final rise in curve 2, resulting in the shift of $\Delta V_{W1/LM}$, which brings about the shift of the peak potential in the VITTM [cf. Eq. 6]. Of course, the ohmic effect, $I_{W1-W2}R$ in Eq. 6, contributes to the shift of the peak potential in the VITTM in addition to the shift of the $\Delta V_{W1/LM}$.

The above consideration may hold even for the shift of the peak potential in the VITTM observed with the BLM.

Conclusion

In the present paper, the transport process of ions from one aqueous medium to another through a BLM was investigated based on the voltammetric concepts and methods, and the process has been demonstrated to be analogous to that through an LM when the BLM as well as two aqueous phases contained sufficient electrolytes, though the BLM is much thinner than the LM. The process is largely due to the concentration of the hydrophilic ion distributed spontaneously into the BLM as the counter ion of the hydrophobic ion added in the aqueous phase, and the concentration is determined by the hydrophobic/hydrophilic natures of both the added and counter ions and the characteristics of the lipid composing the BLM.

The authors wish to thank Professors Tetsuya Hanai and Kouji Asami of Institute for Chemical Research in Kyoto University for their useful comments.

References

1) R. B. Gennis, "Biomembranes," Springer-Verlag, New York (1989), Chaps. 2, 7, and 8.
2) H. T. Tien, "Bilayer Lipid Membranes," Marcel Dekker, New York (1974), Chaps. 1—5.
3) P. Krysinski and H. T. Tien, *Prog. Surf. Sci.*, **23**, 317 (1986).
4) V. K. Miyamoto and T. E. Thompson, *J. Colloid Interface Sci.*, **25**, 16 (1967).
5) E. A. Liberman and V. P. Topaly, *Biochim. Biophys. Acta*, **163**, 125 (1968).
6) Ye. A. Liberman and V. P. Topaly, *Biofizka*, **14**, 452 (1969).
7) R. De Levie, *J. Electroanal. Chem.*, **69**, 265 (1976).
8) O. H. Le Blanc, Jr., *Biochim. Biophys. Acta*, **193**, 350 (1969).
9) L. J. Bruner, *Biophysik*, **6**, 241 (1970).
10) B. Ketterer, B. Neumcke, and P. Läuger, *J. Membr. Biol.*, **5**, 225 (1971).
11) R. De Levie and N. G. Seidah, *J. Membr. Biol.*, **16**, 1 (1974).
12) J. Kutnik and H. T. Tien, *Bioelectrochem. Bioenerg.*, **16**, 435 (1986).
13) O. Shirai, S. Kihara, Y. Yoshida, and M. Matsui, *J. Electroanal. Chem.*, **389**, 61 (1995).
14) H. T. Tien, *Prog. Surf. Sci.*, **19**, 169 (1985).
15) O. Shirai, S. Kihara, M. Suzuki, K. Ogura, and M. Matsui, *Anal. Sci.*, **7th suppl.**, 607 (1991).
16) S. Kihara, M. Suzuki, K. Maeda, K. Ogura, S. Umetani, M. Matsui, and Z. Yoshida, *Anal. Chem.*, **58**, 2954 (1986).
17) K. Ueno, M. Saito, and K. Tamaoku, *Bunseki Kagaku*, **17**, 1548 (1968).
18) J. Chatt and F. A. Hart, *J. Chem. Soc.*, **1960**, 1378.
19) S. Umetani, N. Shigemura, S. Kihara, and M. Matsui, *Talanta*, **38**, 653 (1991).
20) S. Umetani and M. Matsui, *Anal. Chem.*, **64**, 2288 (1992).
21) T. Hanai, D. A. Haydon, and J. Taylor, *Proc. R. Soc. A*, **281**, 377 (1964).
22) T. Hanai, S. Morita, N. Koizumi, and M. Kajiyama, *Bull. Inst. Chem. Res., Kyoto Univ.*, **48**, 147 (1970).
23) H. H. J. Girault and D. J. Schiffrin, in "Electroanalytical Chemistry," "Vol. 15: Electrochemistry of Liquid–Liquid Interface," ed by A. J. Bard, Marcel Dekker, New York (1989).
24) P. Vanysek, in "Lecture Notes in Chemistry," "Vol. 39: Electrochemistry on Liquid/Liquid Interfaces," ed by G. Berthier, M. J. S. Dewar, H. Fischer, K. Fukui, G. G. Hall, J. Hinze, H. H. Jaffe, J. Jortner, W. Kutzelnigg, K. Ruedenberg, and J. Tomasi, Springer-Verlag, Berlin (1985).
25) K. Ogura, S. Kihara, S. Umetani, and M. Matsui, *Bull. Chem. Soc. Jpn.*, **66**, 1971 (1993).
26) H. T. Tien and J. Kutnik, *Photobiochem. Photobiophys.*, **7**, 319 (1984).
27) C. J. Bender and H. T. Tien, *Anal. Chim. Acta*, **198**, 259 (1987).
28) C. J. Bender and H. T. Tien, *Anal. Chim. Acta*, **201**, 51 (1987).
29) C. J. Bender, *Chem. Soc. Rev.*, **17**, 317 (1988).
30) H. T. Tien and A. L. Diana, *J. Colloid Interface Sci.*, **24**, 287 (1967).
31) J. M. Diamond and E. M. Wright, *Ann. Rev. Physiol.*, **31**, 582 (1969).
32) J. M. Diamond and Y. Katz, *J. Membr. Biol.*, **17**, 121 (1974).
33) R. A. Robinson and R. H. Stokes, "Electrolyte Solutions," Butterworth Sci. Pub., London (1959).
34) H. Hauser, D. Oldani, and M. C. Phillips, *Biochemistry*, **12**, 4507 (1973).
35) R. Benz and K. Janko, *Biochim. Biophys. Acta*, **455**, 721 (1976).
36) R. F. Flewelling and W. L. Hubbell, *Biophys. J.*, **49**, 541 (1986).
37) P. Läuger, R. Benz, G. Stark, E. Bamberg, P. C. Jordan, A. Fahr, and W. Brock, *Q. Rev. Biophys.*, **14**, 513 (1981).
38) G. Szabo, *Nature*, **252**, 47 (1974).
39) S. Kihara, *Denki Kagaku*, **63**, 363 (1995).
40) Y. Marcus, *Pure Appl. Chem.*, **55**, 977 (1983).
41) Y. Marcus, M. J. Kamlet, and R. W. Taft, *J. Phys. Chem.*, **92**, 3613 (1988).
42) P. B. Hitchcock, R. Mason, K. M. Tomas, and G. G. Shipley, *Proc. Natl. Acad. Sci. U.S.A.*, **71**, 3036 (1974).
43) H. Hauser, I. Pascher, R. H. Pearson, and S. Sundell, *Biochim. Biophys. Acta*, **550**, 21 (1981).